

Non-Covalent Short Range Interactions

Table of Contents:

1. Motivation	1
2. Short Range Interactions and Surface Forces	1
3. Van der Waals Interactions for Point Interactions	3
4. Surface Forces	4
5. Hamaker Constant	5
6. Van der Waals Retardation Effects	6
7. Adhesion and Surface Energies.....	6
8. Cutoff Distance for Van der Waals Calculations	7
9. Capillary Forces due to Vapor Condensation	8
10. Critical Humidity for Capillary Neck Formation.....	9
11. Estimation of the Tip Radius Utilizing the Capillary Effects	10
12. Modification of Hydrophobicity (Wettability).....	12
13. Force Displacement Curves	13
<i>References</i>	<i>14</i>
<i>Recommended Reading</i>	<i>14</i>

1. Motivation

As technology moves more towards miniaturization in novel product developments, it is imperative to integrate interfacial interactions into design strategies. Consequently, interfacial forces have to be explored. Interfacial forces are on the order of 10^{-6} to 10^{-10} N, strong enough, for instance, to freeze gears in micro-electrical mechanical systems (MEMS), to affect the stability of colloidal system, or to wipe out magnetically stored data information in hard drives. There are multiple ways of exploring the strength of interfacial interactions, one of which is by force spectroscopy, also known as force-displacement (FD) analysis. The FD analysis involves a nanometer sharp scanning force microscopy (SFM) tip that is moved relative to the sample surface in nanometer to micrometer per second, as illustrated at end of this document in Figure 10. Before we discuss FD analysis, we first discuss interaction forces, particularly weak interactions between molecules and solids.

2. Short Range Interactions and Surface Forces

There are three aspects that are of particular importance for any interaction: Its strength, the distance over which it acts, and the environment through which it acts. Short range interactions, as summarized in Table 1, can be of following nature: ionic, covalent, metallic, or dipolar origin. Ionic, covalent, metallic and hydrogen bonds are so-called atomic forces that are important for forming strongly bonded condensed matter. These short range forces arise from the overlap of electron wave functions. Interactions of dipolar nature are classified further into strong hydrogen bonds and weak Van der Waals

(VdW) interactions. They arise from dipole-dipole interactions. Both hydrogen and VdW interactions can be responsible for cooperation and structuring in fluidic systems, but are also strong enough to build up condensed phases. Following is a description of these short range forces:

- A. *Ionic Bonds*: These are simple Coulombic forces, which are a result of electron transfer. For example in lithium fluoride, lithium transfers its 2s electron to the fluorine 2p state. Consequently the shells of the atoms are filled up, but the lithium has a net positive charge and the Fluorine has a net negative charge. These ions attract each other by Coulombic interaction which stabilizes the ionic crystal in the rock-salt structure.
- B. *Covalent Bond*: The standard example for a covalent bond is the hydrogen molecule. When the wave-function overlap is considerable, the electrons of the hydrogen atoms will be indistinguishable. The total energy will be decreased by the “exchange energy”, which causes the attractive force. The characteristic property of covalent bonds is a concentration of the electron charge density between two nuclei. The force is strongly directed and falls off within a few Ångstroms.
- C. *Metallic Bonds and Interaction*: The strong metallic bonds are only observed when the atoms are condensed in a crystal. They originate from the free valence electron sea which holds together the ionic core. A similar effect is observed when two metallic surfaces approach each other. The electron clouds have the tendency to spread out in order to minimize the surface energy. Thus a strong exponentially decreasing, attractive interaction is observed.
- D. *Dipole Interactions*:
 - D.1. Hydrogen Bond Interaction: Strong type of directional dipole-dipole interaction
 - D.2. Van der Waals Interaction: The relevance of VdW interactions goes beyond of building up matter (e.g., Van der Waals organic crystals (Naphthalene)). Because of their “medium” range interaction length of a few Ångstroms to hundreds of Ångstroms, VdW forces are significant in fluidic systems (e.g, colloidal fluids), and for adhesion between microscopic bodies. VdW forces can be divided into three groups:
 - o *Dipole-dipole force*: Molecules having permanent dipoles will interact by dipole-dipole interaction.
 - o *Dipole-induced dipole forces*: The field of a permanent dipole induces a dipole in a non-polar atom or molecule.
 - o *Dispersion force*: Due to charge fluctuations of the atoms there is an instantaneous displacement of the center of positive charge against the center of the negative charge. Thus, at a certain moment, a dipole exists and induces a dipole in another atom. Therefore non-polar atoms (e.g. neon) or molecules attract each other.

Table 1: Short Range Interaction Forces

Nature of Bond	Type of Force	Energy (kcal/mol)	Distance
Ionic bond	Coulombic force	180 (NaCl) 240 (LiF)	2.8 Å 2.0 Å
Covalent bond	Electrostatic force (wave function overlap)	170 (Diamond) 283 (SiC)	N/A
Metallic bond	free valency electron sea interaction (sometimes also partially covalent (e.g., Fe and W))	26 (Na) 96 (Fe) 210 (W)	4.3 Å 2.9 Å 3.1 Å
Hydrogen Bond	a strong type of directional dipole-dipole interaction	7 (HF)	
Van der Waals	(i) dipole-dipole force (ii) dipole-induced dipole force (iii) dispersion forces (charge fluctuation)	2.4 (CH ₄)	significant in the range of a few Å to hundreds of Å

3. Van der Waals Interactions for Point Interactions

The attractive VdW pair potential between point particles (i.e., atoms or small nonpolar spherical molecule) is proportional to $1/r^6$, where r is the distance between the point particles. The widely used semi-empirical potential to describe VdW interactions is the Lennard-Jones (LJ) potential, referred to as the 6-12 potential because of its $(1/r)^6$ and $(1/r)^{12}$ distance r dependence of the attractive interaction and repulsive component, respectively. While the 6-potential is derived from point particle dipole-dipole interaction, the 12-potential is based on pure empiricism. The LJ potential is provided in the following two equivalent forms as function of the particle-particle distance r :

$$\phi(r) = -\frac{C_{vdw}}{r^6} + \frac{C_{rep}}{r^{12}} = 4\epsilon \left[\left(\frac{\sigma}{r}\right)^{12} - \left(\frac{\sigma}{r}\right)^6 \right] \quad (1a)$$

where

$$\sigma = \left(\frac{C_{rep}}{C_{vdw}}\right)^{\frac{1}{6}}; \quad \epsilon = \frac{C_{vdw}^2}{4C_{rep}} \quad (1b)$$

C_{vdw} and C_{rep} are characteristic constants. $C = C_{vdw}$ is called the VdW interaction parameter. The empirical constant ϵ represents the characteristic energy of interaction between the molecules (the maximum energy of attraction between a pair of molecules). σ , a characteristic diameter of the molecule (also called the *collision diameter*), is the distance

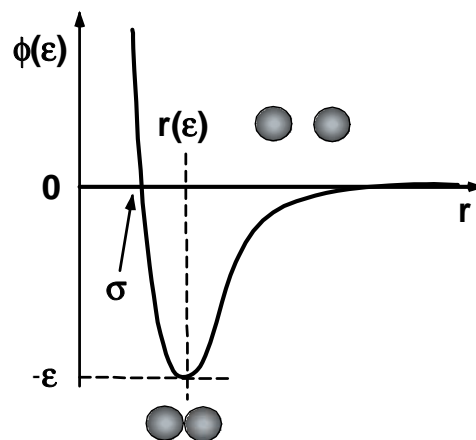


Figure 4: Lennard Jones (6-12) potential (empirical Van der Waals Potential between two atoms or nonpolar molecules).

between two atoms (or molecules) for $\phi(r) = 0$. The LJ potential is depicted in Figure 4..

4. Surface Forces

The integral form of interaction forces between surfaces of macroscopic bodies through a third medium (e.g., vacuum and vapor) are called *surfaces forces*. To apply the VdW formalism to macroscopic bodies, one has to integrate the point interaction form presented above. Consequently, the dipole-dipole interaction strength C but also the exponent of the distance dependence become geometry dependent. For instance, while for point-point particles the exponent is -6, it is -1 and -3 for macroscopic sphere-sphere and sphere-plane interactions, respectively. Thus, while, VdW point particle interactions are very short ranged ($\sim 1/r^6$), macroscopic VdW interactions are long ranged (e.g., sphere-sphere: $\sim 1/D$, where D represents the shortest distance between the two macroscopic objects). Table 3 provides a list of geometry dependent non-retarded VdW interaction strengths and exponents.

In vacuum, the main contributors to long-range surface interactions are the Van der Waals and electromagnetic interactions. At separation distance < 2 nm one might also have to consider short range retardation due to covalent or metallic bonding forces. Van der Waals and electromagnetic interactions can be both attractive or repulsive. In the case of a vapor environment as the third medium (e.g., atmospheric air containing water and organic molecules), one also has to consider modifications by the vapor due to surface adsorption or interaction shielding. This can lead to force modification or additional forces such as the strong attractive capillary forces.

The SFM tip-sample interaction potential W are typically modeled as a sphere-plane interaction, i.e.,

$$W(D) = \frac{-AR}{6D} \quad (2a)$$

with the force

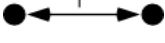
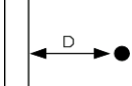

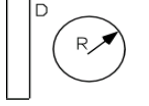
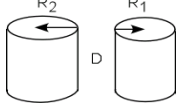
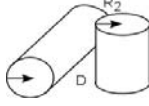
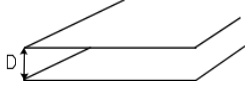
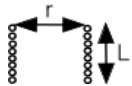
$$-\frac{dW}{dD} = F(D) = \frac{-AR}{6D^2} \quad (2b)$$

where R is the radius of curvature of the tip, and D is the distance between the tip and the plane. The interaction constant A , is called the *Hamaker constant*, defined as $A = \pi^2 C \rho_1 \rho_2$, with the interaction parameter of the point-point interaction C , and the number density of the molecules in both solids ρ_i ($i = 1,2$). The Hamaker constant is based on the mean-field Lifshitz theory. If known, A provides the means to deduce the material specific (i.e., geometry independent) interaction parameter C . Typical values for A , C and ρ are provided in Table 2. Table 3 summarizes the Van der Waals interaction potential for various geometries.

Table 2: Hamaker constants of Hydrocarbon, CCl₄, and water.

Medium	C (10^{-79} Jm^6)	ρ [10^{28} m^{-3}]	A [10^{-19} J]
Hydrocarbon	50	3.3	0.5
CCl ₄	1500	0.6	0.5
Water	140	3.3	1.5

Table 3: Van der Waals interaction Potential

	Geometry of Interaction	Interaction Potential (W)
Point Interaction		Two Atoms $\frac{-C}{r^6}$
		Atom-Surface $\frac{-\pi C\rho}{6D^3}$
Body Interaction		Sphere-Sphere $\frac{-A}{6D} \frac{R_1 R_2}{(R_1 + R_2)}$
		Plane-Sphere $\frac{-AR}{6D}$
		Two Cylinders $\frac{AL}{12\sqrt{2}D^{3/2}} \left(\frac{R_1 R_2}{(R_1 + R_2)} \right)^{1/2}$
		Two Crossed Cylinders $\frac{-A\sqrt{R_1 R_2}}{6D}$
		Plane-Plane $\frac{-A}{12\pi D^2}$
		Two Parallel Chain Molecules $\frac{-3\pi CL}{8\sigma^2 r^5}$

5. Hamaker Constant

Originally the Hamaker constant was determined based on a purely additive method in which polarization was ignored. The Lifshitz theory has overcome the problem of additivity. It is a continuum theory which neglects the atomic structure. The input parameters are the dielectric constants, ϵ , and refractive indices, n . The Hamaker constant for two macroscopic phases 1 and 2 interacting across a medium 3 is approximated as:

$$A \approx \frac{3}{4} kT \left(\frac{\epsilon_1 - \epsilon_3}{\epsilon_1 + \epsilon_3} \right) \left(\frac{\epsilon_2 - \epsilon_3}{\epsilon_2 + \epsilon_3} \right) + \frac{3h\nu_e}{8\sqrt{2}} \frac{(n_1^2 - n_3^2)(n_2^2 - n_3^2)}{\sqrt{(n_1^2 + n_3^2)}\sqrt{(n_2^2 + n_3^2)}\left\{ \sqrt{(n_1^2 + n_3^2)} + \sqrt{(n_2^2 + n_3^2)} \right\}} \quad (3)$$

where ν_e is the absorption frequency (e.g., for H₂O: $\nu_e = 3 \times 10^{15}$ Hz). Table 4 provides non-retarded Hamaker constants determined with the Lifshitz theory (eq. 3).

In general, there is an attractive VDW interaction for $A > 0$, and the two macroscopic phases are attracted to each other. In cases where it is desired to have repulsive forces, the medium must have dielectric properties which are intermediate to the macroscopic phases.

Table 4: Non-retarded Hamaker constants for two interacting media across a vacuum (air) (Source: intermolecular & Surface Forces, J. Israelachvili, Academic Press)³

Medium	Dielectric constant	Refractive Index	Absorption frequency ^a	Hamaker Constant
	ϵ	n	ν (10^{15}s^{-1})	$A_{\text{medium/air/medium}}$ (10^{-20})
Acetone	21	1.359	2.9	4.1
Benzene	2.28	1.501	2.1	5.0
Calcium Flouride	7.4	1.427	3.8	7.0
Carbon tetrachloride	2.24	1.460	2.7	5.5
Cyclohexane	2.03	1.426	2.9	5.2
Ethanol	26	1.361	3.0	4.2
Fused quartz	3.8	1.448	3.2	6.3
Hydrocarbon (crystal)	2.25	1.50	3.0	7.1
Iron oxide (Fe_2O_4)		1.97	3.0 est	21
Liquid He	1.057	1.028	5.9	0.057
Metals (Au, Ag, Cu)			3-5	25-40
Mica	7.0	1.60	3.0	10
n-Pentane	1.84	1.349	3.0	3.8
n-Octane	1.95	1.387	3.0	4.5
n-Dodecane	2.01	1.411	3.0	5.0
n-Tetradecane	2.03	1.418	2.9	5.0
n-Hexadecane	2.05	1.423	2.9	5.1
Polystyrene	2.55	1.557	2.3	6.5
Polyvinyl chloride	3.2	1.527	2.9	7.5
PTFE	2.1	1.359	2.9	3.8
Water	80	1.333	3.0	3.7

^aUV absorption frequencies obtained from Cauchy plots mainly from Hough and White (1980) and H. Christenson (1983, thesis).

6. Van der Waals Retardation Effects

The van der Waals forces are effective from a distance of a few Ångstroms to several hundreds of Ångstroms. When two atoms are a large distance apart, the time for the electric field to return can be critical, i.e., comparable to the fluctuating period of the dipole itself. The dispersion can be considered to be retarded for distances more than 100 Å, i.e., the dispersion energy begins to decay faster than $1/r^6$ ($\sim 1/r^7$). It is important to note that for macroscopic bodies retardation effects are more important than for atom-atom interactions. This is of particular importance for the SFM force displacement method.

7. Adhesion and Surface Energies

The energy of adhesion (or just *adhesion*), W'' , i.e., the energy per unit area necessary to separate two bodies (1 and 2) in contact, defines the interfacial energy γ_{12} as:

$$W'' = 2\gamma_{12}; \quad \gamma_{12} = \gamma_1 + \gamma_2 - 2\sqrt{\gamma_1\gamma_2} \quad (4)$$

where γ_i ($i=1,2$) represent the two surface energies. Assuming two planar surfaces in contact, the Van der Waals interaction energy per unit area is

$$W_1(D) = \frac{-A}{12\pi D^2} \quad (\text{see above}) \quad (5)$$

which was obtained by pairwise summation of energies between all the atoms of medium 1 with medium 2. The summation of atom interactions within the same medium have been neglected, which yields additional energy terms, i.e.,

$$W_2 = -const. + \frac{A}{12\pi D_o^2} \quad (6)$$

consisting of a bulk cohesive energy term (assumed to be constant), and an energy term related to unsaturated "bonds" at the two surfaces in contact (i.e., $D = D_o$). Notice that contact cannot be defined as $D = 0$ due to molecular repulsive forces. D_o is called the "cutoff distance". Hence the total energy of two planar surfaces at a distance $D \geq D_o$ apart is (neglecting the bulk cohesive energy)

$$W = W_1 + W_2 = -\frac{A}{12\pi} \left(\frac{1}{D_o^2} - \frac{1}{D^2} \right) = \frac{A}{12\pi D_o^2} \left(1 - \frac{D_o^2}{D^2} \right). \quad (7)$$

In contact (i.e., $D=D_o$) $W = 0$. In the case of isolated surfaces, i.e., $D = \infty$,

$$W = \frac{A}{12\pi D_o^2}. \quad (8)$$

Thus, in order to separate the two surfaces one has to overcome the energy difference

$$\Delta W = W(D_o) - W(D=\infty) = -\frac{A}{12\pi D_o^2}, \quad (9)$$

which corresponds to the adhesive energy per unit area of $W'' = 2\gamma_{12}$. Hence, the interfacial energy can be expressed as function of the Hamaker constant and the cutoff distance:

$$\gamma_{12} = \frac{A}{24\pi D_o^2}, \quad (10)$$

8. Cutoff Distance for Van der Waals Calculations

The challenge is to determine the repulsive cutoff distance D_o , which unfortunately cannot be set equal to the collision diameter, σ (i.e., the distance between atomic centers). Let us assume a planar solid consisting of atoms that are close-packed. Each surface atom (of diameter σ) will have nine nearest neighbors (instead of 12 as in the bulk). When surface atoms come into contact with a second surface each atom will gain $(12-9)w=3w=3C/\sigma^6$ in binding energy. Thus, the energy per unit area, $S=3w/\sigma^2 \sin(60 \text{ deg}) = \sigma^2 \sqrt{3}/2$, is

$$\gamma_{12} = \frac{1}{2} \left(\frac{3w}{S} \right) = \frac{\sqrt{3}C}{\sigma^8} = \frac{\sqrt{3}C\rho^2}{2\sigma^2}; \quad \rho = \frac{\sqrt{2}}{\sigma^3}, \quad (11)$$

where ρ reflects the bulk atom density for a close packed system. Introducing the definition of the Hamaker constant, it follows

$$\gamma_{12} = \frac{\sqrt{3}C\rho^2}{2\sigma^2} = \frac{\sqrt{3}A}{2\pi^2\sigma^2} \approx \frac{A}{24\pi \left(\frac{\sigma}{2.5} \right)^2}, \quad (12)$$

For $\sigma = 0.4 \text{ nm}$ and $\gamma_{12} = A/(24\pi D_o^2)$ it follows that $D_o = 0.16 \text{ nm}$. $D_o = 0.16 \text{ nm}$ is a remarkable "universal constant" yielding values for surface energies γ that are in good agreement with experiments as shown in the Table 5.

Table 5: Surface energies based on Lifshitz theory and experimental values. (Source: intermolecular & Surface Forces, J. Israelachvili, Academic Press)³

Surface Energy, γ (mJ/m ²)			
Material	A	Lifshitz Theory	Experimental*
	(10 ⁻²⁰)	$A/24 \pi D_o^2$ {D _o =0.165nm}	(20°C)
Liquid helium	0.057	0.28	0.12 - 0.35(at 4-1.6K)
Water	3.7	18	73
Acetone	4.1	20.0	23.7
Benzene	5.0	24.4	28.8
CCl ₄	5.5	26.8	29.7
H ₂ O ₂	5.4	26	76
Formamide	6.1	30	58
Methanol	3.6	18	23
Ethanol	4.2	20.5	22.8
Glycerol	6.7	33	63
Glycol	5.6	28	48
<i>n</i> -Pentane	3.75	18.3	16.1
<i>n</i> -Hexadecane	5.2	25.3	27.5
<i>n</i> -Octane	4.5	21.9	21.6
<i>n</i> -Dodecane	5.0	24.4	25.4
Cyclohexane	5.2	25.3	25.5
PTFE	3.8	18.5	18.3
Polystyrene	6.6	32.1	33
Polyvinyl chloride	7.8	38.0	39

9. Capillary Forces due to Vapor Condensation

In the discussion above we have considered a continuous medium in-between the two surfaces to deduce the surface forces. Thereby, we have assumed that this third medium fills up the vacuum space entirely, i.e., does not introduce interfaces. We have to drop this assumption, however, should the third medium form a finite condensed phase within the interaction zone of the two bodies. Any condensed phase within the interaction zone will exhibit interfaces towards the vapor, and thus, if deformed (e.g., stretched) contribute to the acting forces. These new forces, called *capillary forces*, are on the order of 10⁻⁷ N for single asperity contacts with radii of curvatures below 100 nm.

Capillary forces are meniscus forces due to condensation. It is well known that micro-contacts act as nuclei of condensation. In air, water vapor plays the dominant role. If the radius of curvature of the micro-contact is below a certain critical radius, a meniscus will be formed. This critical radius is defined approximately by the size of the Kelvin radius $r_K = l/(l/r_1 + l/r_2)$ where r_1 and r_2 are the radii of curvature of the meniscus. The Kelvin radius is connected with the partial pressure p_s (saturation vapor pressure) by

$$r_K = \frac{\gamma_L V}{RT \log\left(\frac{p}{p_s}\right)}, \quad (13)$$

where γ_L is the surface tension, R the gas constant, T the temperature, V the mol volume and p/p_s the relative vapor pressure (relative humidity for water). The surface tension γ_L of water is 0.074N/m ($T=20^\circ\text{C}$) leading to a critical Van der Waals distance of water of $\gamma_L V/RT = 5.4 \text{ \AA}$. Consequentially, we obtain for $p/p_s=0.9$ a Kelvin radius of 100 \AA . At small vapor pressures, the Kelvin radius gets comparable to the dimensions of the molecules, and thus, the Kelvin equation breaks down.

The meniscus forces between two objects of spherical and planar geometry can be approximated, for $D \ll R$, as:

$$F^{R \gg D} = \frac{4\pi R \gamma_L \cos \Theta}{(1 + D/d)}, \quad (14)$$

where R is the radius of the sphere, d the length of \overline{PQ} , see Figure 5, D the distance between the sphere and the plate, and θ the meniscus contact angle.

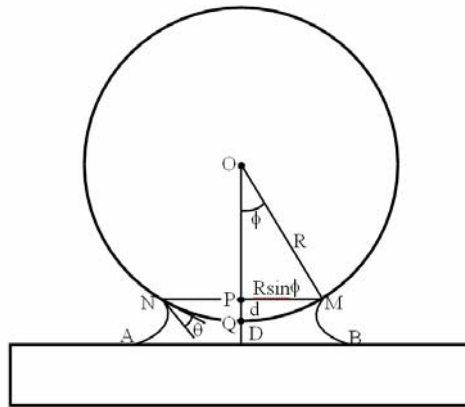


Figure 5: Capillary meniscus between two objects of spherical and planar geometry

The maximum force, found at at $D = 0$ (contact), is $F_{max}^{R \gg d} = 4\pi R \gamma \cos \theta$. While this expression estimates the capillary forces of relatively large spheres fairly accurately, the capillary forces of highly wetted nanoscale spheres requires a geometrical factor K .

$$K = \frac{(1 + \cos \phi)^2}{4 \cdot \cos \phi} \quad (15)$$

where ϕ is the filling angle.

10. Critical Humidity for Capillary Neck Formation

SFM force displacement analysis studies involving hydrophilic counter-surfaces and water vapor have identified three humidity regimes with significantly different involvement of the third medium, as shown in Figure 6. At very low humidity (regime I), below a critical relative humidity (RH) of $\sim 40\%$, no capillary neck is developed, and the forces measured truly reflects VdW interactions. A capillary neck is formed at about 40% RH, which leads to a force discontinuity observed between regimes I and II. We can understand this transition-like behavior of the pull-off force by considering the

minimum thickness requirement of a liquid precursor film for spreading. The height of the precursor film can not drop below a certain minimum, e , which is

$$e = a_0 \left(\frac{\gamma}{S} \right)^{1/2} ; a_0 = \left(\frac{A}{6\pi\gamma} \right)^{1/2} ; S = \gamma_{SO} - \gamma_{SL} - \gamma, \quad (15)$$

where a_0 is a molecular length, S the spreading coefficient, A the Hamaker constant, γ_{SO} the solid-vacuum interfacial energy, and γ_{SL} the solid-liquid interfacial energy. As the water vapor film thickness depends on the RH (i.e., p/p_s), a relative humidity smaller than 40 % does not provide a minimum thickness for the formation of a capillary neck. Once a capillary neck forms between the SFM tip and the substrate surfaces, the pull-off force increases suddenly, and provides over regime II a pull-off force that contains both, VdW and capillary forces. VdW forces from SFM FD analysis as determined, for instance, from regime I, see Figure 6(b), are on the order of 1-10 nN. The capillary force, on the other hand, is on the order of up to 100 nN, and thus, dominates VdW interactions in regime II.

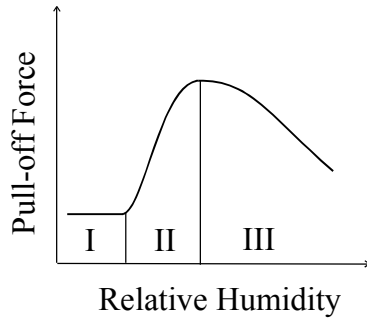


Figure 6(a): Generic sketch of the functional relationship between the pull-off force and the relative humidity (RH). Regimes I, II and III represent the van der Waals regime, mixed van der Waals – capillary regime, and capillary regime decreased by repulsive forces, respectively.

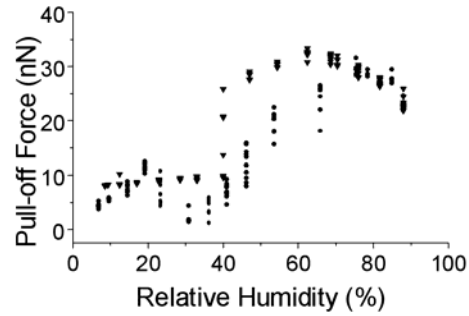


Figure 6(b): Pull-off force vs. RH measured between a hydrophilic silicon oxide SFM tip and a ultra-smooth silicon oxide wafer. ● measured for increasing RH, ▼ measured for decreasing RH. ¹

In the high RH regime (III) the pull-off force decreases with increasing RH for hydrophilic counter-surfaces. At such high humidity, the water vapor film thickness dimensions exceeds the contact size (\rightarrow asperity flooding), and the effect of the capillary interface decreases.

11. Estimation of the Tip Radius Utilizing the Capillary Effects

The capillary effect, commonly not desired, can be useful in estimating the SFM tip radius. Assuming the absence of the flooding effect and the ionic salvation effect within regime III, as discussed in the previous section, the humidity dependent adhesion forces can be described as a mathematical model of sigmoidal form⁴,

$$F_{mea} = (F_{stw} + F_{cap}) + \frac{F_{stw} - (F_{stw} + F_{cap})}{1 + \exp[(\phi_0 - \phi) / m]} \quad (16)$$

where F_{mea} is the experimentally determined pull-off forces,
 F_{stv} is the van der Waals interaction force between the sample and the tip
in water vapor,
 F_{stw} is the van der Waals interaction force between the sample and the tip
in liquid water,
 F_{cap} is the capillary force, ϕ is the relative humidity (in fraction),
 ϕ_0 is the mid-point of the transition regime, and
 m is the transition width.

As shown in Figure 7, the forces, F_{stv} , F_{stw} , and F_{cap} , are components of the measured pull-off force F_{mea} . When the relative humidity is below the transition regime, i.e., $\phi < \phi_0$, the F_{mea} consists F_{stv} only, represents the lower limit of the sigmoidal fit. Above the transition regime, F_{mea} is the sum of F_{stw} and F_{cap} , represents the upper limit of the sigmoidal fit.

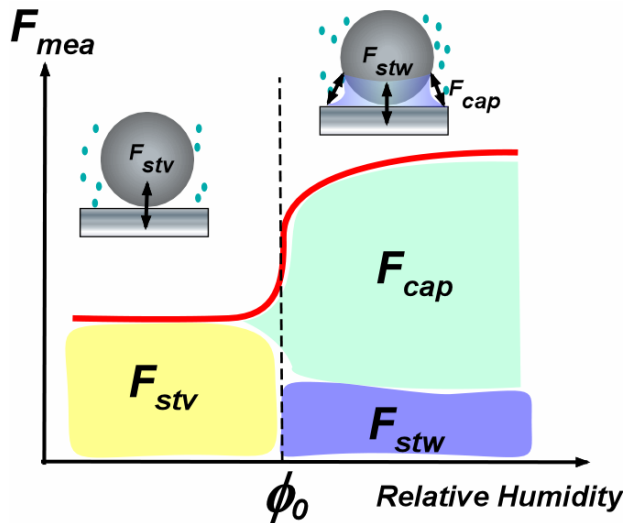


Figure 7: The components of full-off forces in humid environment.

The F_{stw} and F_{stv} can be expressed by assuming that the contact is between an incompressible sphere and a hard flat surface, i.e. Bradley's model (see page 24),

$$F_{stv} = 2\pi \cdot R \cdot W_{stv} \text{ or } F_{stw} = 2\pi \cdot R \cdot W_{stw} \quad (17a \text{ or } 17b)$$

where R is the sphere radius (i.e. SFM tip radius), W is the work of adhesion which is expressed as,

$$W_{ijm} = \gamma_{im} + \gamma_{jm} + \gamma_{ij} \quad (18)$$

where γ is the interfacial energies of the two materials, and i, j, m represents solid i , solid j , and the medium m in which the contact take place, respectively. If the contact is between two solids with the same material, i.e., $i = j$, Eq. (18) reduces to $W_{ijm} = 2\gamma_{im}$.

In order to determine the tip radius R , Eq. (17a) is solved for R using experimentally determined F_{stv} . The R value is then used to determine F_{stw} through Eq. (17b), and F_{cap} is deduced. Employing the geometric coefficient K for the capillary force equation,

$$F_{cap} = 4\pi \cdot R \cdot \gamma_{water} \cos\theta \cdot \frac{(1 + \cos\phi)^2}{4 \cdot \cos\phi} \quad (19)$$

the filling angle ϕ can be deduced. For example, the result obtained by He et. al.¹ on the silicon wafer surface, was analyzed using this model. Using the value of $\gamma_{SiO/air}$ 100 mJ/m²⁵, $\gamma_{SiO/water}$ 24.5 mJ/m²⁵, γ_{water} 72.8 mJ/m², and the contact angle Θ of 0 °, the tip radius R and the filling angle ϕ was determined to be 8.7 nm and 85.6 ° respectively.

12. Modification of Hydrophobicity (Wettability)

Capillary effect is absent when the surface is hydrophobic, i.e., non-wetting, and hydrophobic silicon surfaces can be created with appropriate treatment. In general, the degree of hydrophobicity (wettability) depends on the surface chemistry and micro roughness. One most common technique to measure hydrophobicity is the contact angle measurement. As shown in Figure 8, a droplet of water is placed on a surface of interest and the angle Θ which the water forms with the surface is evaluated. When the angle is smaller than 90 °, the surface is said to be more hydrophilic or wetting. When the angle is larger than 90 °, the surface is rather hydrophobic (non-wetting). The contact angle results from the energy balance between the solid surface, vapor, and the liquid, hence the contact angle, although it is not straightforward, can be used to deduce the surface energy γ . It should be noted that the surface energy (interchangeably called interfacial energy, surface tension), is an important parameter in evaluating the surface forces, as it can be seen in multiple equations presented in previous sections.

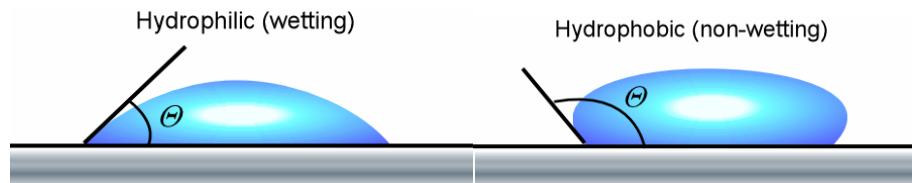


Figure 8: The contact angle measurement. The contact angle Θ is the measure of hydrophobicity (wettability). Left: hydrophilic surface. Right: hydrophobic surface.

The hydrophobicity is a major concern in semiconductor industries, such as IC (integrated circuit) board manufactures and microelectronic technology. Because such devices are used in ambient environment, i.e. humid air, the surfaces are prepared carefully to have both the desired functionalities and the surface characteristics. A silicon wafer is made out of pure silicon, Si, but the surface without any special treatment, is in an oxidized form silicon, SiO_x, a hydrophilic surface. This oxide layer can be etched out by HF (hydrofluoric acid), leaving the surface with hydrogen-terminated silicon, more hydrophobic. Figure 9 is actual photographs of the contact angle measurement on a series of silicon surfaces. Figure 9(b) is as-is silicon surface which is cleaned with organic solvent. This surface is SiO_x covered with residual organic impurities, generating partially wetting (hydrophilic) surface. When the solvent cleaned surface was further treated with UV/Ozone cleaner, which removes the residual organics on the surface, the surface showed complete wetting with the contact angle of 0 °, Figure 9(a). On the other hand, if the surface was treated with HF, the contact angle is rather large ~ 72 °, thus it is rather hydrophobic surface, Figure 9(c). Although this HF treated surface possesses desirable hydrophobicity, the surface is not stable due to its high surface energy. Studies found that the hydrogen-terminated surface in ambient air is oxidized within several hours, resulting in creating naturally grown SiO_x layer on the surface.

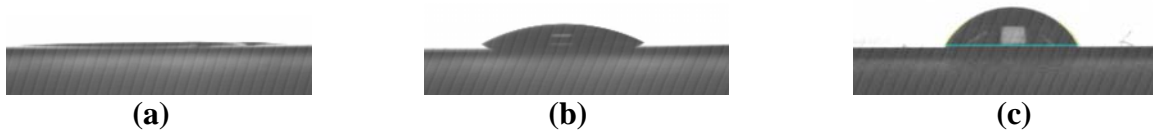


Figure 9: The contact angle measurement of silicon surfaces (a) clean SiOx surface, (b) SiOx covered with organic impurities, (c) HF treated Si surface.

13. Force Displacement Curves

In SFM force displacement (FD) analysis, the normal forces acting on the cantilever are measured as a function of the tip-sample displacement. In other words, the tip-sample distance could not be precisely controlled due to the flexibility of the cantilever. As a result, the FD curve jumps the path of the force curve as illustrated in Figure 10. Figure 10(a) shows the cantilever approach from point D_0 . When the distance reaches point A_0 an instability occurs resulting in a jump into contact to point B_0 . On the retraction out of contact an instability occurs at point C_0 causing the cantilever tip to snap out of contact back to point D_0 . As a result the typical force distance curve is shown in Figure 10(b). Each segment of the curve is described as follows.

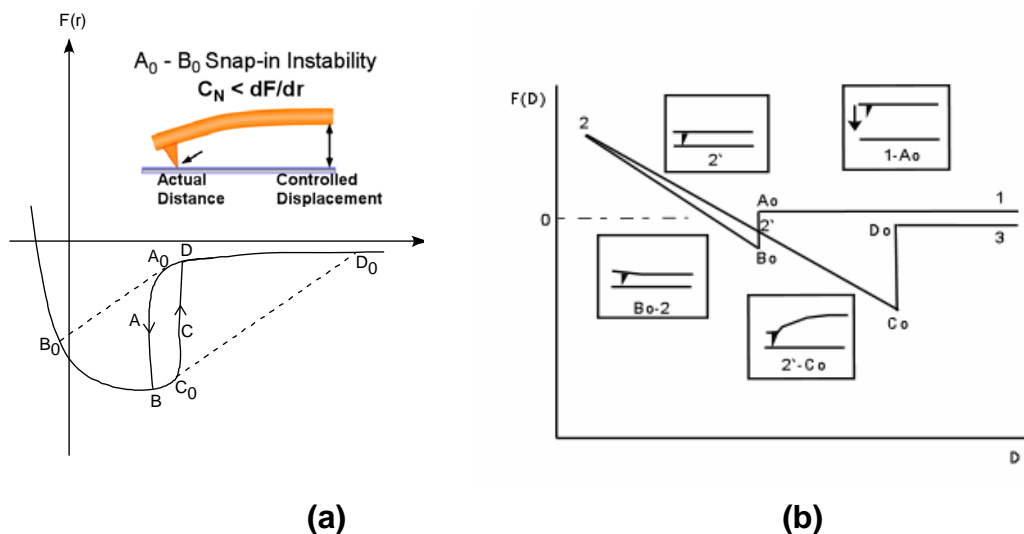


Figure 10: (a) The actual path taken by a SFM cantilever. The inset illustrates the snap-in instability at A_0 where the second derivative of the interaction potential exceeds the spring constant of the cantilever. (b) Typical force distance curve. D = displacement, $F(D)$ = force.

1. *Line 1- A_0 :* The probe and sample are not in contact but the tip is moving toward the sample.
2. *Line A_0 - B_0 :* Jump into contact caused by the attractive van der Waals forces outweighing the force of the cantilever spring between the tip and the sample causing the cantilever to bend.
3. *Line B_0 -2:* Shows upward deflection of the cantilever in response to the sample motion after they are in contact. The shape of the segment indicates whether the sample is deforming in response to the force from the cantilever. (may not always be straight) If the sample is assumed to be a hard surface, the slope of this line is the sensitivity (springiness) of the cantilever.

4. *Line 2-C₀*: As the tip moves away, the slope follows the slope of line B₀-2 closely. If line 2-C₀ is parallel to line B₀-2, no additional information can be determined. However, if there is a difference in the in and out-going curves (hysteresis) gives information on the plastic deformation of the sample. Once it passes point 2', the cantilever begins to deflect downward due to adhesive forces..
5. *Line C₀-D₀*: A jump out of contact occurs when the cantilever force exceeds the adhesive forces.

The jump out of contact distance will always be greater than the jump into contact distance because of few possible causes are:

- a. During contact, some adhesive bonds are created.
- b. During contact, the sample buckles and “wraps” around the tip, increasing the contact area.
- c. Hysteresis contributions
- d. Capillary forces exerted by contaminants such as water.

FD analysis is widely used for adhesion and force interaction studies. Recently biological materials have been studied by force spectroscopy, such as adsorption strength of proteins on a substrate and folding/unfolding energy of DNAs.

References

- ¹ M. He, A. Blum, D. E. Aston, C. Buenviaje, and R. M. Overney, *Journal of chemical physics* **114** (3), 1355 (2001).
- ² H. Hertz, *J. Reine und Angewandte Mathematik* **92**, 156 (1882).
- ³ J. N. Israelachvili, *Intermolecular and surface forces*. (Academic Press, London, 1992).
- ⁴ D. L. Sedin and K. L. Rowlen, *Analytical Chemistry* **72**, 2183 (2000).
- ⁵ C. Ziebert and K. H. Zum Gahr, *Tribology Letters* **17** (4), 901 (2004).
- ⁶ J. A. Greenwood, *Proc. R. Soc. Lond. A* **453**, 1277 (1997).

Recommended Reading

- Contact Mechanics* by K. L. Johnson, Cambridge University Press, Cambridge, 1985.
- Gases, liquids and solids and other states of matter* by D. Tabor, Cambridge Univ. Press, Cambridge, 3rd ed. 2000.
- Intermolecular and surface forces* by J. N. Israelachvili, Academic Press, London, 1992.
- Nanoscience: Friction and Rheology on the Nanometer Scale* by E. Meyer, R. M. Overney, K. Dransfeld, and T. Gyalog, World Scientific Publ., Singapore, 1998.